Bažant, Z.P., and Tsubaki, T. (1980). "Slip-dilatancy model for cracked reinforced concrete." *J. of the Struct. Div.*, Proc. ASCE, 106, 1947–1966.

JOURNAL OF THE STRUCTURAL DIVISION

Slip-Dilatancy Model for Cracked Reinforced Concrete

By Zdeněk P. Bažant,[1] F. ASCE and Tatsuya Tsubaki[2]

Introduction

The stresses transmitted between the opposite surfaces of cracks in concrete have a major effect on the response of reinforced concrete. This has been recognized by Schnobrich and coworkers (18,20) who introduced in finite element analysis the concept of reduced elastic shear stiffness of cracked concrete. The transfer of shear stress across the cracks, due to aggregate interlock, is modeled by multiplying the shear modulus with a certain shear transfer factor α_s such that $0 < \alpha_s < 1$, which is either taken as constant or, more realistically, as a function of the crack width (8,10). This model represents a rather significant advance compared to the previous complete neglect of the shear transfer ($\alpha_s = 0$) and has served as a point of departure for the present work, in which a further improvement is attempted.

The reduction of shear stiffness, however, does not give the full picture. If the opposite surfaces of a rough crack are in contact, and if the normal stress across the crack is zero or constant, any relative tangential displacement δ_t (slip) between the opposite surfaces of a crack is at constant stress always accompanied by a relative normal displacement δ_n (crack width). This is called crack dilatancy. If δ_n is kept constant, slip δ_t leads to jamming of rough crack surfaces (aggregate interlock) which produces not only a shear stress σ^c_{nt} but also a normal compressive stress σ^c_{nn} transmitted across the crack by the contacts of surface asperities. This may be regarded as a manifestation of friction.

Thus, the effect of cracks in concrete cannot be described merely by a reduced shear stiffness $\alpha_s G$ resulting from the relation between δ_t and the shear stress σ^c_{nt} transmitted across the cracks. Rather, it must be described by a relation that involves δ_t, δ_n, σ^c_{nt}, and σ^c_{nn}, i.e., not only tangential but also normal displacement and stress components on a crack (2). A nonlinear model based on tests was developed for this relation (2); it is however unnecessarily sophisti-

Note.—Discussion open until February 1, 1981. To extend the closing date one month, a written request must be filed with the Manager of Technical and Professional Publications, ASCE. This paper is part of the copyrighted Journal of the Structural Division, Proceedings of the American Society of Civil Engineers, Vol. 106, No. ST9, September, 1980. Manuscript was submitted for review for possible publication on August 30, 1979.

[1]Prof. of Civ. Engrg., Northwestern Univ., Evanston, Ill.

[2]Postdoctoral Research Assoc., Northwestern Univ., Evanston, Ill.

cated when a linear structural analysis is carried out, which is normally adequate for the service stress design. Therefore, it is of interest to develop a simpler, linearized model, and we will achieve it by introducing the simple ideas of friction coefficient and dilatancy ratio for the crack slip.

Aside from finite element analysis, our model will also be intended for the design of reinforcement on the basis of given internal forces. Currently, the service stress design (which is required for nuclear structures) is carried out (7) under the assumption that cracks in concrete transmit no shear and normal stresses. This classical design approach, which we will call the frictionless design, represents a correct approach if the cracks indeed have the direction of principal stress in concrete. It must be considered, however, that the stress state which produces the cracks is not the one after the cracks are formed. In fact, the cracks may form even before significant loads are applied, due to shrinkage or temperature changes. Thus, the direction of cracks is highly uncertain and it is a safe practice, as generally accepted for limit analysis (3), to consider that the cracks in concrete may be of any direction.

Is the principal stress direction the most unfavorable one? We will see that usually it is not. This is similar to what has been already discovered for the limit analysis (6), and is due to the fact that crack dilatancy produces extension of reinforcement.

For limit analysis, the frictional approach, which has been verified by analysis of test data (2,5) guarantees proper safety against crack slip; thereby it limits the deformation (especially crack width) preceding failure for cases where the reinforcement direction substantially deviates from the principal direction of internal forces. Similarly, reduction of deformation and crack width as well as a more reliable determination of stresses and deformations may be expected from the frictional service stress design method that we are going to develop. A broader survey of literature may be found in Refs. 2 and 6.

Problem and Basic Assumptions

The concrete is considered to be either in a state of plane stress (slab, plate) or in a state of plane strain, and only the in-plane behavior is considered. Concrete is assumed to contain one or two systems of straight, parallel, equidistant and continuous cracks. We disregard the fact that cracks in concrete often begin to form as a series of discontinuous microcracks and remain such as long as δ_n is very small. The spacing of reinforcing bars as well as the spacing of cracks is assumed to be sufficiently dense so that the change of internal forces from one bar to the next or from one crack to the next would be negligible. At least one principal internal force is assumed to be tensile and concrete is assumed to have no tensile strength. We have to restrict attention to monotonic loading, even though cyclic loading is important and some experiments have recently been carried out (14,15,16,19). To treat the composite action, we assume that the averaged strains in cracked concrete and in the reinforcing net are the same. We will distinguish the case where the opposite crack surfaces are in contact (frictional cracks) from the case where they are not (frictionless cracks). First we consider the frictional cracks.

Stiffness of Concrete with Slipping Frictional Cracks of One Direction

A fundamental property characterizing the response of cracked concrete is

the relationship between the relative normal displacement, δ_n, and the relative tangential displacement, δ_t, between the opposite surfaces of a crack, and the normal stress, σ^c_{nn}, and the shear stress, σ^c_{nt}, that are transmitted across the crack due to contact (or interlock) of concrete surfaces (superscript c refers to concrete) (see Fig. 1). Although this relationship is quite complex and nonlinear (2), we may approximately treat it as friction, writing $|\sigma^c_{nt}| \le -k\sigma^c_{nn} + c$, and if the crack is slipping we have

for $\sigma^c_{nn} \le 0$: $|\sigma^c_{nt}| = -k\sigma^c_{nn} + c$ (frictional slip) . . . . (1)

for $\delta_n \ge 0$: $\delta_n = \alpha_d|\delta_t| + \epsilon$ (dilatancy) . . . . (2)

in which k = friction coefficient; c = cohesion; α_d = dilatancy ratio; and ϵ = expansion (or initial dilatancy).

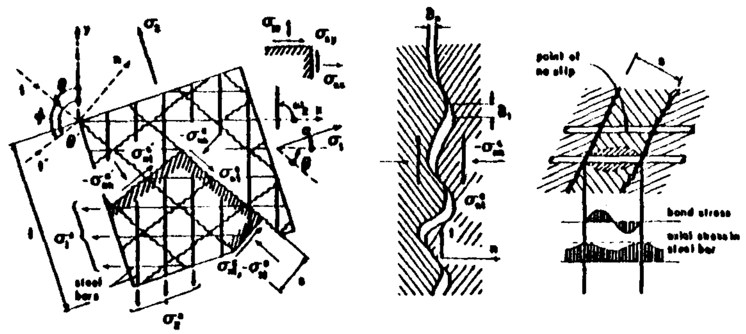

FIG. 1.—Stresses in Cracked Reinforced Concrete: (a) Orthogonally Reinforced Slab; (b) Roughness of Crack Surfaces; (c) Actual Distribution of Stresses

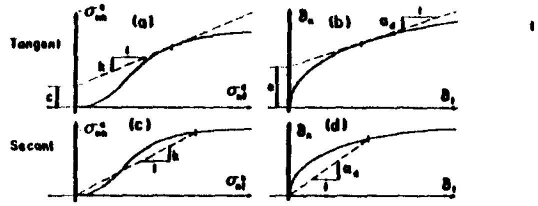

FIG. 2.—Tangent and Secant Linearization of Friction and Dilatancy Laws

In view of the actual nonlinear behavior, k and α_d should be regarded as the slopes of the tangent of some nonlinear diagrams (Fig. 2) of σ^c_{nn} versus σ^c_{nt} and of δ_n versus δ_t, and c and ϵ as the offsets of these tangents on the vertical axes. Optimally, the values for k, α_d, c and ϵ should correspond to the tangents at points close to the actual solution, but in this respect we should keep in mind that the actual diagram of σ^c_{nn} versus σ^c_{nt} is not unique and depends on δ_n, δ_t and the loading history, and the same holds for the diagram of δ_n versus

δ_t. In absence of information on the actual nonlinear behavior, we should use $c = e = 0$.

From the macroscopic point of view, the effect of the relative displacements δ_n and δ_t on many densely distributed parallel cracks of mean spacing, s, is to produce the averaged strains

$$\epsilon^{cr}_{nn} = \frac{\delta_n}{s}; \quad \epsilon^{cr}_{tt} = 0; \quad \gamma^{cr}_{nt} = \frac{\delta_t}{s} \quad \ldots \quad (3)$$

in which γ^{cr}_{nt} = shear angle = twice the tensorial shear strain component ϵ^{cr}_{nt}.

The total strains of concrete containing many densely distributed parallel cracks may then be expressed as

$$\boldsymbol{\epsilon} = \boldsymbol{\epsilon}^c + \boldsymbol{\epsilon}^{cr} \quad \ldots \quad (4)$$

in which $\boldsymbol{\epsilon}^{cr}$ = the column matrix $(\epsilon^{cr}_{nn}, \epsilon^{cr}_{tt}, \gamma^{cr}_{nt})^T$, T denoting a transpose; and $\boldsymbol{\epsilon}$ and $\boldsymbol{\epsilon}^c$ are similar matrices representing the total strains and the strains in the concrete between the cracks. To achieve equilibrium, the stresses in concrete between the cracks must be the same as the stresses transmitted across the cracks. Assuming the concrete between the cracks to be isotropic and elastic, we may then write

$$\boldsymbol{\epsilon}^c = \mathbf{C}_c \boldsymbol{\sigma}^c; \quad \mathbf{C}_c = \begin{bmatrix} E_c^{-1} & -\nu E_c^{-1} & 0 \\ & E_c^{-1} & 0 \\ \text{sym.} & & G_c^{-1} \end{bmatrix} \quad \ldots \quad (5)$$

in which $\boldsymbol{\sigma}^c = (\sigma^c_{nn}, \sigma^c_{tt}, \sigma^c_{nt})^T$; $\mathbf{C}_c$ = the flexibility matrix of uncracked concrete; and E_c, ν, and G_c are Young's modulus, Poisson's ratio, and shear modulus, respectively, of solid concrete that does not contain continuous macroscopic cracks. When the concrete is in a state of plane strain rather than plane stress, E_c and ν must be replaced by $E_c/(1 - \nu^2)$ and $\nu/(1 - \nu)$, respectively.

It must be remembered that Eq. 5 is an acceptable approximation only within the service stress level and that E_c and G_c should be taken as secant moduli. Near ultimate loads, some stress components, e.g., the compression stresses parallel to cracks, may become high even in cracked concrete, and then Eq. 5 would have to be replaced by a nonlinear constitutive relation (e.g., Refs. 1, 3).

If we substitute $\delta_n = s(\epsilon_{nn} - \epsilon^c_{nn})$ and $\delta_t = s(\gamma_{nt} - \gamma^c_{nt})$ (from Eqs. 3 and 4) into Eq. 2, and express ϵ^c_{nn} and γ^c_{nt} from Eq. 5, we get

$$\epsilon_{nn} - \frac{\sigma^c_{nn} - \nu\sigma^c_{tt}}{E_c} = \pm\alpha_d\left(\gamma_{nt} - \frac{\sigma^c_{nt}}{G_c}\right) + \frac{e}{s} \quad \ldots \quad (6)$$

Furthermore, noting that $\epsilon^c_{tt} = \epsilon_{tt}$ and substituting $\sigma^c_{tt} = E_c\epsilon_{tt} + \nu\sigma^c_{nn}$ (Eq. 5) and $\sigma^c_{nt} = \mp k\sigma^c_{nn} \pm c$ (Eq. 1) into Eq. 6, we obtain for slipping cracks

$$\left[\frac{1 - \nu^2}{E_c} + \frac{1}{G_c}(\pm\alpha_d)(\pm k)\right]\sigma^c_{nn} = \epsilon_{nn} + \nu\epsilon_{tt} \mp \alpha_d\gamma_{nt} + \frac{1}{G_c}(\pm\alpha_d)(\pm c) - \frac{e}{s} \quad (7)$$

Among the double signs at k and c, the upper ones go (here and in the sequel) with $\sigma^c_{nt} \geq 0$ and the lower ones with $\sigma^c_{nt} < 0$; as for α_d, the upper signs go with $\delta_t \geq 0$ and the lower ones with $\delta_t < 0$. For admissible solutions the signs of σ^c_{nt} and δ_t must match, and then $(\pm\alpha_d)(\pm k)$ always equals $\alpha_d k$. In a computer program, however, it is not known in advance whether the solution of a certain case will be an admissible one; therefore, the expression $(\pm\alpha_d)(\pm k)$ cannot be replaced by $\alpha_d k$ and must be considered with all sign combinations; the same holds for $(\pm\alpha_d)(\pm c)$.

Expressing σ^c_{nn} from Eq. 7, and substituting this into Eq. 1 and into the relation $\sigma^c_{tt} = E_c\epsilon_{tt} + \nu\sigma^c_{nn}$ (Eq. 5), we finally obtain

$$\boldsymbol{\sigma}^c = \mathbf{D}\boldsymbol{\epsilon} + \mathbf{f} \quad \ldots \quad (8)$$

in which

$$\mathbf{D} = E^* \begin{bmatrix} 1 & \nu & \mp\alpha_d \\ \nu & \dfrac{E_c}{E^*} + \nu^2 & \mp\alpha_d\nu \\ \mp k & \mp k\nu & (\pm\alpha_d)(\pm k) \end{bmatrix}; \quad \mathbf{f} = \begin{Bmatrix} g_1 E^* \\ \nu g_1 E^* \\ \mp k g_1 E^* \pm c \end{Bmatrix} \quad \ldots \quad (9)$$

$$(E^*)^{-1} = \frac{1 - \nu^2}{E_c} + \frac{1}{G_c}(\pm\alpha_d)(\pm k); \quad g_1 = \frac{1}{G_c}(\pm\alpha_d)(\pm c) - \frac{e}{s} \quad \ldots \quad (10)$$

Matrix $\mathbf{D}$ represents the stiffness matrix of concrete containing slipping closely spaced parallel cracks. Note that it is nonsymmetric unless $k = \alpha_d$, which is far from true for concrete. When we use $c = e = 0$, $\mathbf{D}$ is a secant stiffness matrix. For $e = 0$, the value of crack spacing, s, has actually no effect on the resulting stiffness matrix, Eq. 9. (This is not true of the more realistic nonlinear model in Ref. 2.) Note also that matrix $\mathbf{D}$ is singular because the last row is a multiple of the first row and the last column is a multiple of the first column. This singularity is an inevitable consequence of adopting the friction and dilatancy laws (Eqs. 1 and 2) for approximating the relation among σ^c_{nn}, σ^c_{nt}, δ_n and δ_t. When this relation is modeled more accurately, the incremental stiffness matrix is obtained as nonsingular (2), but the theory becomes more complex. We will see that the singularity of $\mathbf{D}$ causes no problem when we deal with reinforced concrete because the stiffness matrix of the composite is nonsingular.

A very important property is the cross effect between ϵ_{nt} and σ^c_{nn} or between ϵ_{nn} and σ^c_{nt}. These cross effects influence the response profoundly. They cause the principal directions of stress in concrete and those of strain not to coincide, while in the currently used approach these directions do coincide.

Stiffness of Concrete with Slipping Frictional Cracks of Two Directions

Reinforced concrete may contain parallel crack systems of two directions. The angle between the two crack systems, generally nonorthogonal, will be denoted as ϕ (see Fig. 1), and all quantities referring to the second crack system will be labeled by primes. For the second system we again have:

$$\text{for} \quad \sigma^{c'}_{nn} \leq 0; \quad |\sigma^{c'}_{nt}| = -k'\sigma^{c'}_{nn} + c'; \quad \ldots \quad (11)$$

$$\text{for} \quad \delta'_n \geq 0; \quad \delta'_n = \alpha'_d|\delta'_t| + e' \quad \ldots \quad (12)$$

We allow k', α'_d, c', and e' to be in general different from k, α_d, c, and e, so as to admit that the diagrams in Fig. 2 could be linearized about different points.

Superimposing the strains due to cracks in both directions and transforming the primed strains due to the second crack system to the coordinates of the first crack system, we get

$$\epsilon^{cr}_{nn} = \frac{\delta_n}{s} + \frac{\delta'_n}{s'}\cos^2\phi - \frac{\delta'_t}{2s'}\sin 2\phi\ ;\quad \epsilon^{cr}_{tt} = \frac{\delta'_n}{s'}\sin^2 2\phi + \frac{\delta'_t}{2s'}\sin 2\phi \quad (13)$$

$$\gamma^{cr}_{nt} = \frac{\delta_t}{s} + \frac{\delta'_n}{s'}\sin 2\phi + \frac{\delta'_t}{s'}\cos 2\phi \quad (14)$$

Also, by coordinate transformation

$$\sigma^{c'}_{nn} = \sigma^c_{nn}\cos^2\phi + \sigma^c_{tt}\sin^2\phi + \sigma^c_{nt}\sin 2\phi \quad (15)$$

$$\sigma^{c'}_{nt} = -\frac{1}{2}(\sigma^c_{nn} - \sigma^c_{tt})\sin 2\phi + \sigma^c_{nt}\cos 2\phi \quad (16)$$

Substitution of these expressions into Eq. 1 and Eq. 11 yields

$$\sigma^c_{tt} = f_1\sigma^c_{nn} + f_2 \quad (17)$$

in which

$$f_1 = \frac{1}{f_0}\left[\frac{1}{2}\sin 2\phi \pm k\cos 2\phi \mp k'\cos^2\phi + (\pm k)(\pm k')\sin 2\phi\right];$$

$$f_2 = \frac{1}{f_0}\left[\pm c' \mp c\cos 2\phi - (\pm k')(\pm c)\sin 2\phi\right];\quad f_0 = \frac{1}{2}\sin 2\phi \pm k'\sin^2\phi \quad (18)$$

From Eqs. 4, 5, 13, and 14, we have

$$\frac{\delta_n}{s} = \epsilon_{nn} - \frac{\delta'_n}{s'}\cos^2\phi + \frac{\delta'_t}{2s'}\sin 2\phi - \frac{1}{E_c}(\sigma^c_{nn} - \nu\sigma^c_{tt}) \quad (19)$$

$$\frac{\delta_t}{s} = \gamma_{nt} - \frac{\delta'_n}{s'}\sin 2\phi - \frac{\delta'_t}{s'}\cos 2\phi - \frac{1}{G_c}\sigma^c_{nt} \quad (20)$$

Substitution of Eqs. 19, 20, and 12 into Eq. 2 yields

$$\delta'_t = \frac{1}{f_3}\left\{\pm\alpha_d\left(\gamma_{nt} - \frac{\sigma^c_{nt}}{G_c}\right) - \left(\epsilon_{nn} - \frac{\sigma^c_{nn} - \nu\sigma^c_{tt}}{E_c}\right) + \frac{e}{s} + \frac{e'}{s'}\left[\cos^2\phi - (\pm\alpha_d)\sin 2\phi\right]\right\} \quad (21)$$

in which

$$f_3 = \frac{1}{s'}\left\{\pm\alpha_d\cos 2\phi \mp \alpha'_d\cos^2\phi + \left[\frac{1}{2} + (\pm\alpha_d)(\pm\alpha'_d)\right]\sin 2\phi\right\} \quad (22)$$

Eqs. 4, 5, and 13 provide

$$\epsilon_{tt} = \frac{1}{s'}\left(\pm\alpha'_d\sin^2\phi + \frac{1}{2}\sin 2\phi\right)\delta'_t + \frac{1}{E_c}(\sigma^c_{tt} - \nu\sigma^c_{nn}) + \frac{e'}{s'}\sin^2\phi \quad (23)$$

Substituting Eqs. 21, 1, and 17 into Eq. 23, we get

$$\sigma^c_{nn} = E^*(\epsilon_{nn} + f_4\epsilon_{tt} \mp \alpha_d\gamma_{nt} + f_5) \quad (24)$$

in which

$$(E^*)^{-1} = \frac{1}{E_c}\{1 - \nu f_1 + f_4(f_1 - \nu)\} + \frac{1}{G_c}(\pm\alpha_d)(\pm k) \quad (25)$$

$$f_4 = \frac{\pm\alpha_d\cos 2\phi \mp \alpha_d\cos^2\phi + \left[\frac{1}{2} + (\pm\alpha_d)(\pm\alpha'_d)\right]\sin 2\phi}{\pm\alpha'_d\sin^2\phi + \frac{1}{2}\sin 2\phi} \quad (26)$$

$$f_5 = \frac{f_2}{E_c}(\nu - f_4) + \frac{1}{G_c}(\pm\alpha_d)(\pm c) - \frac{e}{s} - \frac{e'}{s'}(\cos^2\phi \mp \alpha_d\sin 2\phi + f_4\sin^2\phi) \quad (27)$$

Finally, Eqs. 24, 17, and 1 yield the stress-strain relation in Eq. 8 with

$$\mathbf{D} = E^*\begin{bmatrix} 1 & f_4 & \mp\alpha_d \\ f_1 & f_1f_4 & \mp\alpha_d f_1 \\ \mp k & \mp kf_4 & (\mp\alpha_d)(\mp k)\end{bmatrix};\quad \mathbf{f} = \begin{Bmatrix} f_5E^* \\ f_1f_5E^* + f_2 \\ \mp kf_5E^* \pm c\end{Bmatrix} \quad (28)$$

Note that this stiffness may be written also in the form $\mathbf{D} = E^*\mathbf{a}^T\mathbf{b}$ in which $\mathbf{a} = (1, f_1, \mp k)$; and $\mathbf{b} = (1, f_4, \mp\alpha_d)$. This indicates that matrix $\mathbf{D}$ is again singular. We may further observe that the cross effects between shear stress and normal strain and between shear strain and normal stress are again present and the matrix is nonsymmetric. Note also that the values of crack spacings s and s' have no effect on $\mathbf{D}$.

For the special case where the first crack system is oriented in the principal strain direction (i.e., we have frictionless no-slip cracks), the concrete is subjected to uniaxial compression parallel to the first crack system, and if the second crack system is slipping, it must form with the first system an angle ϕ such that $\pm\cot\phi = k'$ = friction coefficient. Calculations of deformations due to the second crack system yield an expression for the uniaxial compression stiffness parallel to the first crack system, as reduced by the presence of the second crack system. However, since the secant uniaxial stiffness in compression is well known from tests, it is preferable to assess it directly.

The case where both crack systems are in the principal strain directions (frictionless cracks) is a trivial one. Concrete can then transmit no stress and the applied loads must be alined with bar directions or else such cracks could not exist.

In our treatment of the simultaneous slip on two crack systems we neglect the effects of the mismatch at crack corners (Fig. 3(*c*)). For the simultaneous slips, δ_t and δ_t', to occur at zero normal relative displacements, δ_n and δ_n', the triangles of sides δ_t and δ_t' at crack corners would overlap (according to our assumed simple kinematics) and the corners would have to get sheared off, crushed, and removed. This effect should be negligible for small enough δ_t and δ_t' because the area of the triangles to be sheared off $(\delta_t \delta_t')$ is second-order small, and so should be the normal and shear resultants from these triangles as compared to σ^c_{nt} or σ^c_{nn}.

To avoid crack corner overlap and shear-off, the slips δ_t and δ_t' would have to be accompanied by additional dilatancies, $\Delta\delta_n = \delta_t/2$ and $\Delta\delta_n' = \delta_t'/2$, as shown in Fig. 3(*e*). We therefore propose that the way to account for crack corner overlap is to consider increased values of dilatancy factors α_d and α_d' whenever there is simultaneous slip on two crack systems. Because the ratio of the sides of corner triangles to the total crack length is δ_t or δ_t', we may consider that

$$\alpha_d = \alpha_d^* + c_d |\delta_t'| \quad \text{(29)}$$

in which α_d^* = the dilatancy ratio when a single crack system slips; c_d = an

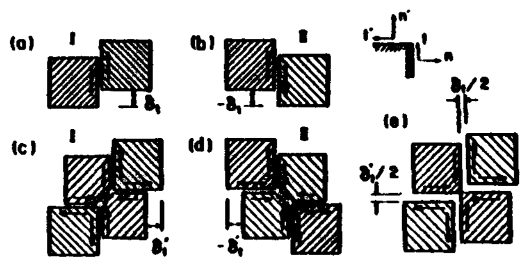

FIG. 3.—Possible Crack Slip Patterns (a–d) and Additional Dilatancy due to Corner Overlap (e)

empirical positive constant; and δ_t' = the slip of the other crack system. However, the correction $c_d |\delta_t'|$ is small and negligible for small enough slips.

Stiffness of Concrete Containing Contactless Cracks or Nonslipping Cracks in Contact

If there is only one system of open cracks the surfaces of which have no contact, Eq. 2 must be replaced by an inequality, $\delta_n > \alpha_d |\delta_t| + \epsilon \; (> 0)$, and Eq. 3 must be omitted because the strains due to cracks, ϵ^{cr}, are indeterminate. Further we must replace the friction law, Eq. 1, with the conditions $\sigma^c_{nn} = 0$, $\sigma^c_{nt} = 0$.

Eq. 4 reduces to the relation $\epsilon^c_{tt} = \sigma^c_{tt}/E_c$. Thus, the stiffness matrix of concrete with one system of contactless cracks (Eq. 9) has the form

$$\mathbf{D} = \begin{bmatrix} 0 & 0 & 0 \\ 0 & E_c & 0 \\ 0 & 0 & 0 \end{bmatrix} \quad \text{(30)}$$

This matrix differs from that presently used for cracked concrete (18) by the bottom diagonal term for shear, which is here taken as zero rather than $\alpha_s G_c$.

It is interesting to note that the matrix **D** for concrete with contacting cracks (Eq. 9) yields the matrix **D** for contactless cracks (Eq. 30) as a limiting case for $k \to \infty$, $\alpha_d \to \infty$ (at $k/\alpha_d \sim$ constant), except that the last diagonal coefficient of the resulting matrix is obtained as G_c rather than 0. However, this coefficient is irrelevant when we seek the crack direction for which the shear strain is zero.

If the crack surfaces are in contact but do not slip, the cracked concrete behaves just like uncracked (solid) concrete and its incremental stiffness matrix is, under the assumption of linearity, given by Eq. 5, i.e.,

$$\mathbf{D} = \mathbf{C}_c^{-1} \quad \text{(contact, no-slip)} \quad \text{(31)}$$

Application to Finite Element Analysis

Matrix **D** from Eqs. 9 or 28 may be used as the incremental (tangent) stiffness matrix in finite element analysis with successive small loading steps. For steps in which the crack direction is already known the following rules are suggested.

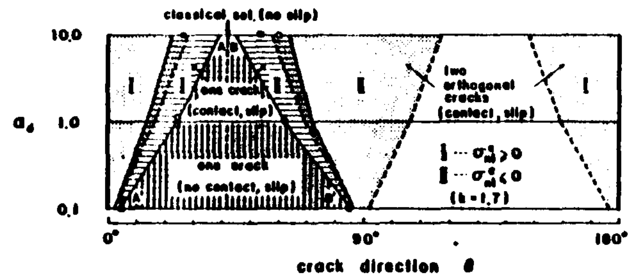

FIG. 4.—Type of Solution for Various Crack Angles, θ, and Dilatancy Ratios, α_d (Overall Maxima of Stresses in Reinforcement (Solid Circles) and Concrete (Open Circles), and Crack Width (Squares); on Lines AA′ and BB′, $\sigma^c_{nt} = \sigma^c_{nn} = 0$)

Case 1. If there has been slipping contact in the preceding loading step, i.e., $c - k\sigma^c_{nn} = \pm\sigma^c_{nt}$ and $\delta_n = \epsilon \pm \alpha_d \delta_t$ with certain of these signs, we assume contact with slip of the same sign for the current loading step. However, (a) if we get slip δ_t of opposite sign we must switch to assuming contact with slip of opposite sign; (b) if we violate $\sigma^c_{nn} \le c/k$ for the end of the current loading step, we must switch to the case of no contact; and (c) if we violate $\delta_n \ge \epsilon$ for the end of the current loading step, we must switch to the case of contact without slip (Eq. 31).

Case 2. If there has been no contact in the preceding step, i.e., $\delta_n > \alpha_d |\delta_t| + \epsilon$ and $\sigma^c_{nn} = 0$, we assume the same for the current loading step, but if we violate $\delta_n > \alpha_d |\delta_t| + \epsilon$ in which $\delta_n = s(\epsilon_{nn} - \epsilon^c_{nn})$ and $\delta_t = s(\gamma_{nt} - \gamma^c_{nt})$ for the end of the current step, we switch to the case of slipping contact with the same sign of δ_t.

Case 3. If there has been contact without slip in the preceding loading step (Eq. 31), we assume the same for the current step, but if we violate σ^c_{nn} <

c/k (0 if $c = 0$) we switch to the case of slipping contact with the same sign of σ^c_{nt}.

Unless an explicit step-by-step algorithm is used, we should iterate calculation of the step with the corrected assumption. The rules for two crack systems must exhaust all combinations of the foregoing cases.

In the foregoing procedure, we disregard for the sake of simplicity the possibility that a solution may exist for more than one case (verified by Fig. 4). The conditions stated for cases 1(b), 1(c), 2, and 3 result from Eqs. 1 and 2 upon noting that $|\sigma^c_{nt}| \geq 0$ and $|\delta_t| \geq 0$. It might be preferable to replace them by the conditions $\sigma^c_{nn} \leq 0$ and $\delta_n \geq 0$, but then we would lose continuity between cases 1 and 2 or 1 and 3 if $c \neq 0$ or $e \neq 0$.

The case of no contact (case 2) is in reality obtained only if $\delta_t = 0$ (see Ref. 2); however, in view of the simplifying Eq. 2 we must allow in case of no contact a finite range of δ_t, as stated for case 1.

Stiffness of Cracked Reinforced Concrete

If the cracks are densely distributed so that the change of stress from one crack to another is not large, we may consider that, by reasons of symmetry, the bars do not slip within concrete at the midpoints between two adjacent parallel cracks [Fig. 1(c)]. Elsewhere there may be bond slip between the bars and concrete, and we know that each bar must actually exhibit bond slip within a certain distance (bond slip length) from the surface of crack because the elasticity solution indicates an infinite bond stress at the surface of the crack. The average strains in the reinforcement are determined by the displacements of the aforementioned midpoints at which there is no bond slip, and these strains must be the same as the macroscopic strains, ϵ_{nn}, ϵ_{tt} and ϵ_{nt}, of the cracked concrete.

The average axial strains in the bars may be determined as

$$\epsilon_i = \epsilon_{nn} \cos^2 (\omega_i - \theta) + \epsilon_{tt} \sin^2 (\omega_i - \theta) + \frac{1}{2} \gamma_{nt} \sin 2(\omega_i - \theta) \quad \text{(32)}$$

The macroscopic stresses, σ^s_i, resulting from the axial forces in the steel bars per unit area of reinforced concrete (not of steel) are

$$\sigma^s_i = E_s p_i \epsilon_i \quad \text{(33)}$$

in which ϵ_i = axial strain in the ith system of steel bars; E_s = Young's modulus of steel bars; and p_i = percentage of reinforcement, i.e., cross-section area of steel per unit area of the reinforced concrete slab.

It is possible to include in Eq. 33 the apparent increase of stiffness of reinforcement due to the interaction with concrete. Between the cracks, the concrete adjacent to the steel bar is forced by bond stresses to extend together with steel. This may be treated as if the cross-section area of steel, i.e., p_i, increased by a transformed cross-section area of a layer of concrete of a certain thickness around the bar. However, in the numerical calculations this effect was neglected for lack of precise information, which is on the safe side.

Writing the axial stiffness matrices of the bars in the n-t coordinate system, and summing them, we obtain the combined stiffness matrix due to the axial stiffness of all bars:

$$\mathbf{D}^s = \sum_{i=1}^{N} \mathbf{R}_i^T \mathbf{D}_i^s \mathbf{R}_i \quad \text{(34)}$$

in which

$$\mathbf{D}_i^s = \begin{bmatrix} p_i E_s & 0 & 0 \\ 0 & 0 & 0 \\ 0 & 0 & 0 \end{bmatrix}, \quad \mathbf{R}_i = \begin{bmatrix} c^2 & s^2 & cs \\ s^2 & c^2 & -cs \\ -2cs & 2cs & c^2 - s^2 \end{bmatrix} \quad \text{(35)}$$

Here $c = \cos(\omega_i - \theta)$ and $s = \sin(\omega_i - \theta)$. For an orthogonal net we have $N = 2$, $\omega_1 = 0°$, $\omega_2 = 90°$. The combined stiffness of cracked reinforced concrete is $\mathbf{D} + \mathbf{D}^s$, which follows from the relation $\sigma = \sigma^c + \sigma^s = (\mathbf{D} + \mathbf{D}^s)\epsilon$, in which $\sigma = (\sigma_{nn}, \sigma_{tt}, \sigma_{nt})^T$ = column matrix of total stresses.

Maximum Stresses in Concrete and Steel and Crack Width

The basic principle generally adopted in the design of reinforced concrete is that the structure must be safe for cracks of *any* orientation. In our case of a regular reinforcing net, we must, therefore, try all possible crack angles, θ, and determine the critical angle, θ_{cr}, for which maximum effects are obtained. Different values of θ_{cr} must be expected for the attainment of maxima of various design parameters, e.g., the stress in one or the other steel bar system, the maximum principal stress in concrete, or the crack width. A computer program (4) has been set up to determine θ_{cr} and the maximum effects for a concrete plate of a given thickness and given reinforcement, subjected to given loads. The loads are given as prescribed principal internal forces of inclination α (see Fig. 1).

Because the calculations are inexpensive, the maxima are found in the program simply by scanning the entire range of θ. A series of discrete values of θ, increasing from 0° to 180° by steps of 1° or 0.1°, is selected. The stresses and crack width are solved for each of them, and the cases giving the maximum values are located among the results. The flow scheme of the program (4) is organized as follows.

1. Data input (material constants, reinforcement percentages and angles, principal total stresses σ_1, σ_2 in the reinforced slab and their inclination, α, etc.). Initialize the arrays for storing the maximum stresses and maximum crack width.
2. Start loop on discrete crack angles θ, incremented by $\Delta\theta$ from 0° to 180°.
3. For each θ, solve the displacements and stresses for all possible cases: (a) One frictionless crack without contact (classical approach); (b) one frictional slipping crack: (I) $\delta_t \geq 0$ and $\sigma^c_{nt} \geq 0$, or (II) $\delta_t \leq 0$ and $\sigma^c_{nt} \leq 0$; (c) two frictional slipping cracks: (I) $\delta_t \geq 0$, $\sigma^c_{nt} \geq 0$ and $\delta'_t \leq 0$, $\sigma^{c'}_{nt} \leq 0$, or (II) $\delta_t \leq 0$, $\sigma^c_{nt} \leq 0$ and $\delta'_t \geq 0$, $\sigma^{c'}_{nt} \geq 0$; and (d) crack in contact without slip ($\delta_n = \delta_t = 0$), equivalent to no crack. (The case of two cracks, cases a and b combined, is not considered for reasons explained after Eq. 28.) In each

case select the proper signs in front of k, k', α_d, and α'_d. Then set up the stiffness martix of cracked reinforced concrete and solve Eq. 38 for strains. Then calculate the stresses and relative displacements on the crack.

4. Check the solution.

Case a—one frictionless crack without contact: $\delta_n > \alpha_d|\delta_t| + e$? Also store $|\delta_t|$ = minimum for all discrete angles θ considered so far (to find θ for which $\delta_t = 0$, which is the classical case.)

Case b—one frictional slipping crack: $\sigma^c_{nn} \leq 0$? and (I) $\delta_t \geq 0$ and $\sigma_{nt} \geq 0$?; or (II) $\delta_t \leq 0$ and $\sigma_{nt} \geq 0$?

Case c—two frictional slipping cracks: $\sigma^c_{nn} \leq 0$, $\sigma^{c'}_{nn} \leq 0$? and (I) $\delta_t \geq 0$, $\sigma^c_{nt} \geq 0$? and $\delta'_t \leq 0$, $\sigma^{c'}_{nt} \leq 0$?; or (II) $\delta_t \leq 0$, $\sigma^c_{nt} \leq 0$? and $\delta'_t \geq 0$, $\sigma^{c'}_{nt} \geq 0$?

Case d—crack in contact without slip: $\sigma^c_{nn} \leq 0$? (at $\delta_t = 0$). For all cases, $\sigma^c_1 \leq 0$? (i.e., the maximum principal stress in concrete must be compressive). This implies the check $\sigma^c_{tt} \leq 0$? for the frictionless crack. (Note that Eq. 1 requires only $\sigma^c_{nn} \leq c/k$ for case a, but we prefer $\sigma^c_{nn} \leq 0$.) If any one of the conditions for the particular case is violated, the solution for this case is inadmissible; discard it.

5. Check for all foregoing cases whether the admissible solutions of stresses in reinforcement and concrete and the crack width exceed the previously attained maxima for any of the particular cases, and if they do, store the new maxima and record the corresponding θ.

6. Go to step 2 unless all discrete angles θ have been considered.

7. Print maxima and corresponding angles θ, and stop.

As we see from this algorithm, the problem of solving the stresses in concrete and reinforcement and the deformations of cracked reinforced concrete for given total stresses is a rather complex nonlinear optimization problem with many linear inequality constraints. The constraints are due to the linearizations achieved by the concepts of friction and dilatancy, and to the neglect of tensile strength of concrete. The solution nonetheless requires fewer material parameters than the full nonlinear incremental solution of the problem (2) in which these constraints do not appear. Whereas the classical solution for frictionless cracks in principal strain direction can be calculated by hand (7), the inclusion of friction and dilatancy requires a computer. However, the solution by computer (4) is very inexpensive.

The classical approach (7) admits a solution only for one certain crack angle θ, whereas frictional cracks admit solutions for a finite and broad range of angles θ (see Fig. 4). Thus the condition of maximum possible stresses or crack width is indispensable for having a unique solution.

Calculation of the crack width requires knowledge of the crack spacing, which may be estimated from experience. Theoretical prediction involves two effects. One is the transmission of tension from bars into concrete by bond stresses; another is stability and unstable localization of strain into cracks. Study of these problems is beyond the scope of this paper.

Numerical Studies and Analysis of Results

When the reinforcement is oriented along the principal stresses, frictionless

cracks normal to the reinforcement represent a feasible solution and are, in fact, the governing case. Thus, the difference between the frictional analysis and the classical frictionless analysis may be expected to increase as the angle, α, between the reinforcement and the principal stresses increases, and this is indeed verified by numerical calculations. We select here an example where, as we shall see, the difference is significant: $\alpha = 30°$; applied principal stresses $\sigma_1 = 1.0$, $\sigma_2 = 0.5$; $\omega_1 = 0°$, $\omega_2 = 90°$ (orthogonal reinforcing net); $p_1 = p_2 = 0.01$ (reinforcement ratios); $E_c = 1.0$; $\nu = 0.18$; $E_s = 7.0$, and we use crack spacing $s = 1$. We treat E_c, E_s, σ_1, σ_2, and s as dimensionless. We will explore the solutions for various k and α_d. For lack of experimental evidences and for simplicity we assume that the coefficients characterizing the cracks are constant, and we set $k' = k$, $\alpha'_d = \alpha_d$, $s' = s$, $c = c = e = 0$. For the solutions shown here, the crack angle has been incremented in the program (4) usually by $\Delta\theta = 0.1°$, but for Fig. 6 by 1°.

The results for the maximum stresses in reinforcement and concrete and for the maximum crack width, δ_n, which are maximum with respect to crack angles and various cases and sign combinations, are plotted in Fig. 5. They are given in terms of their ratios to the maximum values of the maximum reinforcement stress, σ^s_0, the maximum principal compression, σ^c_1, in concrete, and the maximum crack width, δ_{n0}, that are obtained for frictionless cracks in principal strain direction (7). It is noteworthy that in many cases this ratio is much larger than 1.0 and that the smallest values are obtained when $\alpha_d \simeq 1$.

What are the proper values for k and α_d? No precise experimental information exists but a crude estimate can be made. It seems appropriate to select values that correspond to the load at which the cracks begin to slip and open significantly. According to tests $k \simeq 1.7$ when the crack surfaces exhibit large slip (17). Examination of the calculated response curves based on a theory that was calibrated by several test series (2) indicates also that $k \simeq 1.7$ and, moreover, $\alpha_d \simeq 1.0$. The value $\alpha_d = k$ which would correspond to a symmetric stiffness matrix (and to a normality rule of plasticity) is definitely inapplicable.

For these typical values, the maximum stress in reinforcement is about 18% larger than the value for the classical frictionless approach [see Fig. 5(*a*) and (*b*)]; the maximum principal stress in concrete (for any crack angle) is over 30% larger [Fig. 5(*c*) and (*d*)] and the maximum crack width is about 8% larger (Fig. 5(*e*) and (*f*). These corrections are certainly significant. Similarly to the limit analysis with crack friction (6), we thus find that a neglect of friction on the cracks is not on the safe side.

Although, for some crack angles θ, the case of two crack systems prevails over the case of a single crack system, the maximum values for all crack angles are always given by a single crack system. This is shown by Fig. 6, in which $\phi = 0$ corresponds to a single crack system.

As shown in Fig. 4, the range of angles θ (between the first cracks and the major reinforcement) for which frictional slipping cracks exist strongly depends on α_d although it is almost independent of k. The range becomes narrower as α_d decreases, and for $\alpha_d \leq 0.01$ no admissible solution with slipping frictional cracks is found (if $\Delta\theta = 0.1°$ is used) and all solutions consist of contactless cracks.

Note in Fig. 4 that the maxima of steel stress, of principal compression

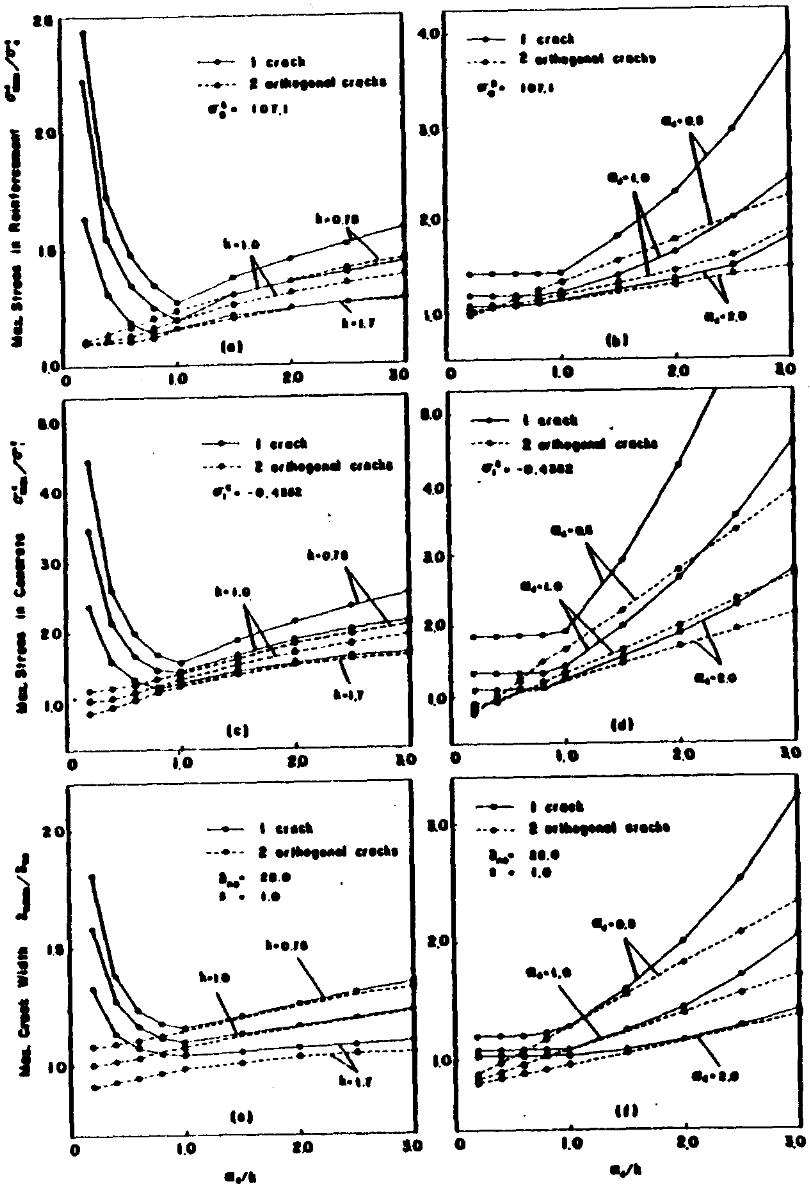

FIG. 5.—Maximum Values of Stresses in Reinforcement, Magnitude of Principal Compression in Concrete, and Crack Width (*a, c, e*: constant = k; *b, d, f*: constant = α_d)

magnitude in concrete, and of crack width for a typical α_d (and $e = 0$) occur at a crack angle which considerably differs from the principal strain direction (assumed in the classical approach) and typically corresponds to a transition from the case of contactless slipping crack ($\delta_t \neq 0$) to the case of frictional slipping cracks, i.e., $\delta_n/|\delta_t| = \alpha_d$ (for $e = 0$) and $\sigma^c_{nn} = \sigma^c_{nt} = 0$. Thus, the friction coefficient k has (for typical α_d) no effect on these maxima. This is certainly an interesting result, for in limit frictional analysis (6) the value of k has a major effect while α_d does not enter the solution.

The crack angles that lead to maximum steel stress and maximum concrete stress or crack width are normally rather different. For very high α_d, the maxima

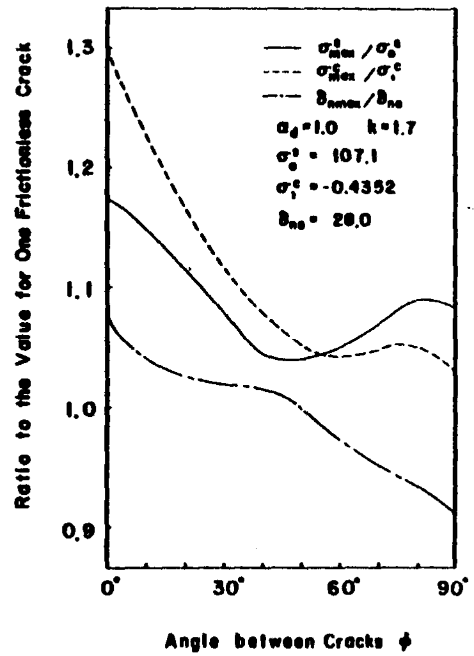

FIG. 6.—Influence of Angle between Two Cracks upon Maximum Stresses in Reinforcement, Principal Compression Magnitude in Concrete, and Crack Width

can occur for slipping cracks with $\sigma^c_{nt} \neq 0$. The classical case of cracks in principal strain direction gives nearly minimum (rather than maximum) crack width δ_n.

The ranges of crack angle for various types of solution and the calculated maximum stresses and crack widths for these ranges are summarized in Table 1. A single preexisting crack for the blank domain in Fig. 4 does not permit any admissible solution; neither do two slipping cracks in contact. This simply means that a crack of a different angle will be produced by the load, and the preexisting crack will behave as frictional without slip.

Thus, we see that consideration of dilatancy is essential if we want to account

1. The concepts of secant friction coefficient and dilatancy ratio for the interlocked cracks in reinforced concrete lead to a simple stiffness matrix for cracked reinforced concrete (Eq. 9 or 28) which is suitable for finite element analysis.

2. The relations for friction and dilatancy make the crack stiffness matrix singular; but this causes no problem because the stiffness of the reinforcement makes the total stiffness matrix of cracked reinforced concrete nonsingular.

3. The resulting stiffness matrix is in general nonsymmetric unless the dilatancy ratio equals the friction coefficient, which is far from true for cracks in concrete at the onset of large crack slip.

4. As in the currently used stiffness matrix (18), the shear transfer due to aggregate interlock on the cracks is accounted for. The present stiffness matrix is, however, more realistic as it also accounts for friction and dilatancy on the cracks. This leads to cross terms relating shear stress (or strain) to normal strain (or stress) that are absent in the currently used matrix, and causes the principal stress and strain to be non-coaxial.

5. In the present service stress design, and similarly for the frictional limit design, the principal strain direction (frictionless crack without contact) is not the most unfavorable crack direction, unless the reinforcement is laid in the principal direction.

6. For the present "service stress design with crack slip," the maximum steel and concrete stresses and crack width are never smaller than for the classical service stress design without crack slip. If the angle of reinforcement with the principal stress direction is between 20° and 45°, these maxima are significantly larger (while they are nearly the same if the angle is less than 10°). This is a safer design approach, which is particularly important for nuclear structures.

7. For orthogonal nets, the maxima of steel stress, of principal compression magnitude in concrete, and of crack width (for $\epsilon = 0$) are obtained for the case of a single crack system, normally with a large slip. For typical dilatancy ratios (and $\epsilon = 0$) they occur at a crack angle at which the case of contactless slipping cracks ($\delta_t \neq 0$) transits into the case of frictional slipping cracks. Thus, the maxima are characterized by vanishing stresses ($\sigma^c_{nt} = \sigma^c_{nn} = 0$) with the crack-width-to-slip ratio equal to the dilatancy ratio ($\delta_n/|\delta_t| = \alpha_d$ for $\epsilon = 0$). Therefore, the friction coefficient, k, normally has no effect on these maxima, while the dilatancy ratio, α_d, has a major effect; this is contrary to the situation in frictional limit analysis. For very high dilatancy ratios, however, the maxima can occur for slipping cracks with nonzero frictional stress. Moreover, the maximum stress in the second bar system occurs, even for typical α_d, for the case of frictional slipping cracks. Thus, the case of frictional slip cannot be omitted. The crack angles that lead to maximum steel stress and maximum concrete stress or crack width are normally rather different.

8. For crack angles other than those leading to maximum stresses and crack width, the results are strongly influenced not only by the dilatancy ratio, α_d, but also by the friction coefficient, k. The classical frictionless solution without crack slip is obtained as the limiting case if both the friction coefficient and the dilatancy ratio tend to infinity.

9. The case of two intersecting crack systems generally gives higher values of stresses and displacements than the classical solution, i.e., a single system of contactless (frictionless) cracks in principal strain direction ($\delta_t = 0$). This classical case also gives nearly the smallest (not largest) value of crack width, δ_n. The present method gives significantly higher stresses than the classical frictionless design without crack slip only when the direction of reinforcement substantially deviates from the principal stress direction. These are cases for which unduly large deformations and crack width have been observed in practice.

10. The present method also allows the design for a specified crack width, provided that the crack spacing is known.

11. When there are two crossing crack systems, the overlap of crack corners and their shear-off are neglected in the calculations. This effect could be accounted for by an increased value of the dilatancy ratio, compared to the case of a single crack system, but no tests to determine it are known.

12. Bond slip of steel bars may be approximately accounted for by an increased apparent stiffness of the steel bars (tension stiffening effect).

13. Dowel action of steel bars crossing the crack has been neglected in calculations although it is no doubt significant. A method to account for it is proposed, but the material coefficients are as yet unknown.

14. Although the effects of friction and dilatancy are based on test results (2), no test data seem to exist to verify our deductions for reinforcing nets. Such test data are needed.

Acknowledgment

Support of the National Science Foundation under Grant ENG75-14848-A01 to Northwestern University is gratefully acknowledged. The first author also obtained partial support under Guggenheim Fellowship awarded to him for 1978-79. Ted B. Belytschko of Northwestern University is thanked for some useful suggestions.

Appendix.—References

1. Bažant, Z. P., and Bhat, P., "Endochronic Theory of Inelasticity and Failure of Concrete," *Journal of the Engineering Mechanics Division*, ASCE, Vol. 102, No. EM4, Proc. Paper 12360, Apr., 1976, pp. 331–344.
2. Bažant, Z. P., and Gambarova, P., "Rough Cracks in Reinforced Concrete," *Journal of the Structural Division*, ASCE, Vol. 106, No. ST4, Proc. Paper 15330, Apr., 1980, pp. 819–842.
3. Bažant, Z. P., and Kim, S.-S., "Plastic-Fracturing Theory for Concrete," *Journal of the Engineering Mechanics Division*, ASCE, Vol. 105, No. EM3, Proc. Paper 14653, June, 1979, pp. 407–428.
4. Bažant, Z. P., and Tsubaki, T., "Computer Program NET77 for Evaluating Regular Reinforcing Nets in Concrete," *Structural Engineering Report No. 79-7/640c*, Northwestern University, Evanston, Ill., 1980; obtainable from National Information Service for Earthquake Engineering-Computer Applications, University of California, Berkeley, Calif.
5. Bažant, Z. P., and Gambarova, P., "Ductility and Failure of Net-Reinforced Concrete Shell Walls," *Transactions*, Fifth International Conference on Structural Mechanics in Reactor Technology, West Berlin, Aug., 1979, Paper J4/9, T. A. Jaeger and B. A. Boley, eds., North Holland, Amsterdam.
6. Bažant, Z. P., and Tsubaki, T., "Concrete Reinforcing Net: Optimum Slip-Free Limit Design," *Journal of the Structural Division*, ASCE, Vol. 105, No. ST2, Proc. Paper 14344, Feb., 1979, pp. 327–346; and also Bažant, Z. P., Tsubaki, T., and Belytschko, T. B., "Concrete Reinforcing Net: Safe Design," *Journal of the Structural Division*,

ASCE, Vol. 106, No. ST9, Proc. Paper 15705, Sept., 1980, pp. 1899–1906.

7. Duchon, N. B., "Analysis of Reinforced Concrete Membrane Subject to Tension and Shear," *American Concrete Institute Journal*, Vol. 69, No. 9, Sept., 1972, pp. 578–583.
8. Fardis, M. N., and Buyukozturk, O., "Shear Transfer Model for Reinforced Concrete," *Journal of the Engineering Mechanics Division*, ASCE, Vol. 105, No. EM2, Proc. Paper 14507, Apr., 1979, pp. 255–275.
9. Jiminez-Perez, R., Gergely, P., and White, R. N., "Shear Transfer across Cracks in Reinforced Concrete," *Report 78-4, Dept. of Structural Engineering*, Cornell University, Ithaca, New York, Aug., 1978.
10. Leombruni, P., Buyukozturk, O., and Connor, J. J., "Analysis of Shear Transfer in Reinforced Concrete with Application to Containment Wall Specimens," *Research Report R79-26, Structures Publication No. 648*, Dept. of Civil Engineering, Massachusetts Institute of Technology, Cambridge, Mass., June, 1979.
11. Marchertas, A. H., Fistedis, S. H., Bažant, Z. P., and Belytschko, T. B., "Analysis and Application of Prestresses Concrete Reactor Vessels for LMFBR Containment," *Nuclear Engineering and Design*, Vol. 49, 1978, pp. 155–173.
12. Mattock, A. H., and Hawkins, N. M., "Shear Transfer in Reinforced Concrete—Recent Research," *Journal of the Prestressed Concrete Institute*, Vol. 17, No. 2, Mar./Apr., 1972, pp. 55–75.
13. Mattock, A. H., "Shear Transfer in Concrete Having Reinforcement at an Angle to the Shear Plane," *Shear in Reinforced Concrete*, Special Publication SP-42, American Concrete Institute, Detroit, Mich., 1974, pp. 17–42.
14. Mattock, A. H., "The Shear Transfer Behavior of Cracked Monolithic Concrete Subject to Cyclically Reversing Shear," *Report SM74-4*, Dept. of Civil Engineering, University of Washington, Seattle, Wash., Nov., 1974.
15. Mattock, A. H., "Shear Transfer under Cyclically Reversing Loading, across an Interface between Concretes Cast at Different Times," *Report SM77-1*, Dept. of Civil Engineering, University of Washington, Seattle, Wash., June, 1977.
16. Oesterle, R. G., and Russell, H. G., "Shear Tests on Reinforced Concrete Membrane Elements," presented at the April 2–6, 1979, ASCE Convention & Exposition and Continuing Education Program, held at Boston, Mass. (Preprint 3594).
17. Paulay, T., and Loeber, P. J., "Shear Transfer by Aggregate Interlock," *Shear in Reinforced Concrete*, Special Publication SP-42, American Concrete Institute, Detroit, Mich., 1974, pp. 1–15.
18. Suidan, M., and Schnobrich, W. C., "Finite Element Analysis of Reinforced Concrete," *Journal of the Structural Division*, ASCE, Vol. 99, No. ST10, Proc. Paper 10081, Oct., 1973, pp. 2109–2122.
19. White, R. N., and Holley, M. J., "Experimental Studies of Membrane Shear Transfer," *Journal of the Structural Division*, ASCE, Vol. 98, No. ST8, Proc. Paper 9145, Aug., 1972, pp. 1835–1852.
20. Yuzugullu, O., and Schnobrich, W. C., "A Numerical Procedure for the Determination of the Behavior of a Shear Wall Frame System," *American Concrete Institute Journal*, Vol. 70, No. 7, July, 1973, pp. 474–479.

ABSTRACT: A model is presented to calculate stresses, deformations, and crack width for a concrete slab or a shell wall that carries in-plane forces and is reinforced by a dense regular net of steel bars and containing one or two systems of straight, parallel, equidistant, and densely distributed cracks. Friction on the cracks (aggregate interlock) and dilatancy due to their slip is approximately taken into account, and slipping cracks without contact are also allowed. The resulting stiffness matrix for concrete with frictional cracks is nonsymmetric and involves cross-terms relating the shear stress (or strain) and the normal strain (or stress), which implies that the principal strains and stresses in concrete are not co-axial. The proposed "service stress design with crack slip" never predicts smaller values of stresses in steel and concrete and of crack width than the classical frictionless design without crack slip. Significantly larger values are obtained when the angle between steel bars and principal stress is large. A single system of slipping cracks in contact is found to be always the critical case for maximum stresses and crack width.

JOURNAL OF THE
STRUCTURAL DIVISION

Slip-Dilatancy Model for Cracked Reinforced Concrete

By Zdeněk P. Bažant,[1] F. ASCE and Tatsuya Tsubaki[2]

Introduction

The stresses transmitted between the opposite surfaces of cracks in concrete have a major effect on the response of reinforced concrete. This has been recognized by Schnobrich and coworkers (18,20) who introduced in finite element analysis the concept of reduced elastic shear stiffness of cracked concrete. The transfer of shear stress across the cracks, due to aggregate interlock, is modeled by multiplying the shear modulus with a certain shear transfer factor α_s such that $0 < \alpha_s < 1$, which is either taken as constant or, more realistically, as a function of the crack width (8,10). This model represents a rather significant advance compared to the previous complete neglect of the shear transfer ($\alpha_s = 0$) and has served as a point of departure for the present work, in which a further improvement is attempted.

The reduction of shear stiffness, however, does not give the full picture. If the opposite surfaces of a rough crack are in contact, and if the normal stress across the crack is zero or constant, any relative tangential displacement δ_t (slip) between the opposite surfaces of a crack is at constant stress always accompanied by a relative normal displacement δ_n (crack width). This is called crack dilatancy. If δ_n is kept constant, slip δ_t leads to jamming of rough crack surfaces (aggregate interlock) which produces not only a shear stress σ^c_{nt} but also a normal compressive stress σ^c_{nn} transmitted across the crack by the contacts of surface asperities. This may be regarded as a manifestation of friction.

Thus, the effect of cracks in concrete cannot be described merely by a reduced shear stiffness $\alpha_s G$ resulting from the relation between δ_t and the shear stress σ^c_{nt} transmitted across the cracks. Rather, it must be described by a relation that involves δ_t, δ_n, σ^c_{nt}, and σ^c_{nn}, i.e., not only tangential but also normal displacement and stress components on a crack (2). A nonlinear model based on tests was developed for this relation (2); it is however unnecessarily sophisti-

Note.—Discussion open until February 1, 1981. To extend the closing date one month, a written request must be filed with the Manager of Technical and Professional Publications, ASCE. This paper is part of the copyrighted Journal of the Structural Division, Proceedings of the American Society of Civil Engineers, Vol. 106, No. ST9, September, 1980. Manuscript was submitted for review for possible publication on August 30, 1979.

[1] Prof. of Civ. Engrg., Northwestern Univ., Evanston, Ill.
[2] Postdoctoral Research Assoc., Northwestern Univ., Evanston, Ill.